Proceedings of the ASME 2010 3rd Joint US-European Fluids Engineering Summer Meeting and 8th International Conference on Nanochannels, Microchannels, and Minichannels
FEDSM-ICNMM2010
August 1-5, 2010, Montreal, Canada

FEDSM-ICNMM2010-30341

3-D NUMERICAL SIMULATION OF GAS-LIQUID FLOW IN A MINICHANNEL WITH A NON-UNIFORM GDL SURFACE

Yulong Ding[1], Xiaotao T. Bi[1], David P. Wilkinson[1]

1. Department of Chemical and Biological Engineering, Clean Energy Research Centre, University of British Columbia
2360 East Mall Vancouver, BC, Canada, V6T 1Z3

ABSTRACT

Gas-liquid two-phase flow in rectangular minichannels of polymer-electrolyte membrane fuel cells (PEMFCs) has a major impact on the fuel cell performance and durability. Different from traditional two-phase flow in other applications, water in the PEMFCs is introduced into the minichannel from the gas diffusion layers (GDLs) through random pores of different sizes. Meanwhile, the four channel surfaces may have different wettabilities due to the different materials used. Thus, the microstructure of GDLs and the surface wettability should be considered in investigating the two-phase flow in PEMFC channels. One challenge in simulating PEMFCs is that, full consideration of detailed microstructure of GDL needs extremely large computational time. In this work, we simplified the microstructure of GDL to a number of representative pores on the 2D GDL surface. A 3-D minichannel with 1.0 mm × 1.0 mm square cross section and 100 mm long was used in the simulation. Operating conditions and material properties were selected according to realistic fuel cell operating conditions. Volume of fluid (VOF) method was employed to explicitly track the droplet surfaces emerging from the non-uniform GDLs. Simulation results show that, as the flow develops along the channel, the flow pattern evolves from corner flow on the bottom and side wall to corner flow on the top wall, annular flow and slug flow. The effects of liquid injection rates were studied, and it is found that the high liquid flow rate would accelerate the flow pattern development. The effect of wall surface material wettability was also studied by changing the hydrophobicity of GDL surface and side walls, separately. Simulation results show that the material wettability has a strong impact on the two-phase flow pattern, with a more hydrophilic side walls and/or a more hydrophobic GDL surface being more beneficial for expelling water out of the channel.

INTRODUCTION

Fuel cells show great potential as an alternative energy-conversion device. Among different types of fuel cells, polymer-electrolyte membrane fuel cells (PEMFCs) have been receiving the most attention for their low operating temperatures (60~90^{o}C), simple design and low costs. Water management is a key issue to improve the performance of PEM fuel cells. The excess liquid water, generated by electrochemical reaction, leading to so-called "flooding", would block the reaction sites in the catalyst layers or block the diffusion pathway of reactants, causing a negative effect on the fuel cell performance. Moreover, the existing liquid water may also result in gas-liquid two-phase flow in gas flow channels. Due to the particularity of PEM fuel cells, such as two-phase flow simultaneously with mass transfer, heat transfer and electrochemical reactions, different material properties in different components, and water emerging from non-uniform GDL surface, the gas-liquid flow in PEM fuel cell channels is quite different from conventional two-phase flow in mini/micro channels. Great attention has been given to two-phase flow in PEM fuel cells recently, both experimentally and computationally [1]. It is found that the two-phase flow in the gas flow channels has a major impact on the performance and durability of PEMFCs. Thus, it is essential to fundamentally understand the gas-liquid two-phase flow behavior in PEM fuel cell channels.

Computational modeling and simulation are one of the powerful tools to better understand the two-phase flow in PEM fuel cells due to its low cost and easy implementation. Since 2000s, two-phase models began to be incorporated in the fuel

cell modeling [2]. Early two-phase flow models always assumed the liquid water moving at the same velocity as the gas flow, called mist flow (e.g. [3, 4]. However, in-situ experiment results showed that at high current densities, water emerging from GDL surface formed droplets rather than mists [5]. Thus, the droplets behavior in gas flow channels should be well understood to minimize its detrimental effect on PEM fuel cell performance. Recent years, volume of fraction (VOF) method became popular in modeling gas-liquid flow in PEM fuel cell channels due to its capacity to consider surface tension and wall adhesion effects and also its ability to track the interface between the two phases. Thus, liquid droplets behaviors can be captured explicitly. A lot of modeling work based on VOF method has been published with both droplets formation and motion being investigated both in two-dimensional and three-dimensional flows [5-7]. Parametric studies on effects of material wettability, gas or liquid velocity, contact angle hysteresis and surface tension were also reported [6, 8-13]. Novel gas flow channel designs have also been explored using VOF method [14-17]. VOF method was even coupled with electrochemical reaction, heat transfer and species transport to model a PEM fuel cell unit [18, 19]. However, none of these studies considered the microstructure of GDL surface. They treated the GDL surface either as a homogenous surface or a surface with only one pore opened for liquid water injection.

In our previous work [20], a simplified microstructure of GDL surface was proposed in simulating gas-liquid two-phase flow in microchannels of PEMFCs by changing the pore diameter and the number of pore openings on the GDL surface. It was found that, in the channel width direction, at least 2 pores are required to represent the microstructure of the GDL surface, and the two-phase flow pattern in the channel does not change with further reduction in the pore diameter. In this work, we extend the previous work by implementing the simplified microstructure in a minichannel, which is comparable with realistic PEMFC gas flow channels. The two-phase flow patterns in the minichannel, effects of liquid injection rates and surface wettabilities were investigated in the simulations.

NUMERICAL METHOD

The three dimensional computational domain is shown in Figure 1. This cuboid channel, which is used in all the simulations, has a 1.0 mm × 1.0 mm square cross section and 100 mm in length with a hydrophobic GDL surface on the bottom and three hydrophilic channel walls. Air flows into the channel from one end and liquid water is injected from multiple pores opened on the GDL surface. 320 pores with the same diameter of 450 μm are located on the GDL surface, corresponding to the simplified microstructure of GDL surface proposed in our previous work [20] (Figure 2).

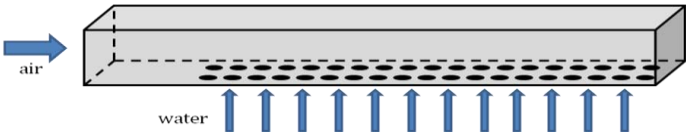

Figure 1. Three dimensional computational domain.

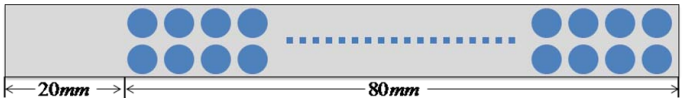

Figure 2. Non-uniform GDL surface.

For the base case, the velocity of air is set at 5 m/s at atmospheric pressure, which is of the same order of magnitude as flows encountered in automotive fuel cell stacks [11]. The liquid injection velocity is 10^{-4} m/s for all the pores, which is according to the theoretical calculation of liquid generation rate at a current density of 0.5 A/cm^2. Laminar flow regime and non-slip boundary condition are used since the Reynolds number of each phase is quite small (Re_g=458, Re_l=11.9). Static contact angle of GDL surface and channel wall surface is set at 140^o and 45^o respectively, based on typical PTFE treated carbon paper GDL materials [21]. The time step for the baseline simulation is set at 10^{-6} s, which ensures that the global courant number is much less than 1.

The VOF method used in all the simulation was implemented using a commercial software, FLUENT® 6.3.26. All the governing equations could be found in its user's guide [22]. The geometric reconstruction scheme is used to interpolate the two-phase interface.

RESULTS AND DISCUSSION

Two-phase flow patterns in minichannel

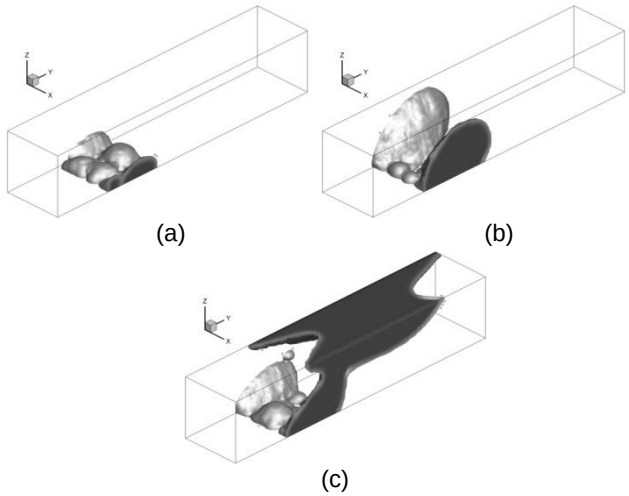

Figure 3. Three stages of the emerging water droplet into a microchannel: (a) merging, (b) accumulating, (c) detaching. [20]

In our previous work, the two-phase flow pattern in a microchannel (250μm×250μm×1250μm) with a simplified

microstructure of GDL surface was investigated using the VOF method. Three stages of two-phase flow patterns were identified, namely emergence and merging of liquid water on the GDL surface, accumulation on the side walls, and detachment from the top wall (See Figure 3).

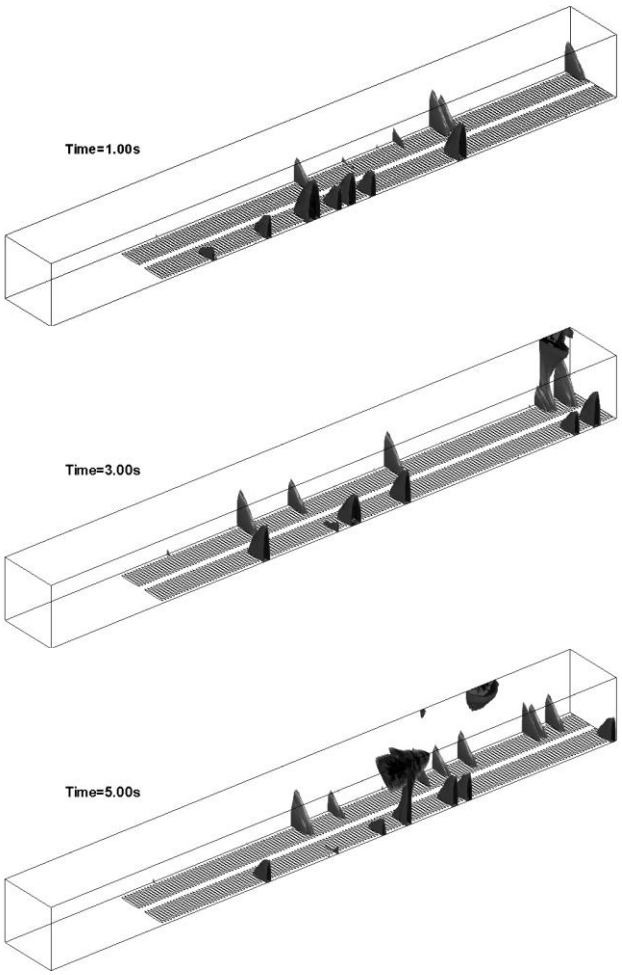

Figure 4. Two-phase flow patterns in the minichannel.

This three-stage flow pattern is also identified in the base case of current simulation (See Figure 4). It is worth noting that since the length to height ratio of the channel is 100:1 the length of the channel is suppressed 10 times to give a better overview of the whole channel. Therefore, the circle pores become ellipsed in Figure 4. Liquid droplets emerging from the pores coalesce on the GDL surface. Due to the wettability difference between the GDL surface and channel walls, liquid water tends to accumulate on the side walls, which results in the formation of large droplets (emergence and merging stage). Then, these droplets move slowly along the side walls due to the drag force exerted by the gas, which forms so-called "corner flow" on the GDL surface (bottom corner). As these droplets move forward, more and more droplets coalesce and result in even larger droplets, which move faster along the channel (accumulating stage). Once these droplets hit the top wall, they rapidly spread out on the top wall, and, due to their much faster speed, quickly detach themselves from the droplets on the bottom corner, with some water on the side wall also being dragged away (detachment stage). As a result, a corner flow on the top wall is formed. Since the droplets on the top wall move faster than those on the bottom corner, they have more opportunities to coalesce with other droplets sitting on the bottom corner. Therefore, they are usually larger than those on the bottom corner. It is also seen that the emergence and merging stage and the accumulating stage occur continuously in the channel, but the detachment only occurs periodically.

Effects of liquid flow rates

In the base case, the liquid injection rate is set according to the theoretical liquid generation rate by the electrochemical reaction at cathode side catalyst layer, and the gas is dry air. Practically, the inlet gas is humidified to increase the membrane conductivity. Therefore, the liquid water formation rate in the cathode side channel usually is much higher than that of generated by the reaction due to the water condensation. In this section, the effects of liquid flow rates are investigated by amplifying the liquid flow rate by 10(10x case), 100(100x case) and 1000(1000x case) times, respectively.

The two-phase flow patterns for each case are shown in Figure 5. For the base case (1x case), as shown in the previous section, the two-phase flow pattern is corner flow, with liquid flowing mostly along the bottom corners, and occasionally along the top corners. As the liquid injection rate increases, e.g. in the 10x case, more droplets emerge into the minichannel. Therefore, bigger droplets are formed due to the more frequent coalescence occurring on the bottom corner, which also makes it easier to form the top corner flow. Further increasing the liquid flow rates, e.g. in the 100x case, results in more liquid water flowing on the top wall and forming a continuous liquid film on the top wall due to the hydrophilic channel side and top walls. The flow pattern in this case is close to annular flow, except that more water on the top and less water on the bottom walls. For the last case, liquid flow rate is amplified by 1000 times. At the beginning of the channel, the liquid water almost blocks the whole cross section of the channel. Due to the density difference between the gas and liquid, it is easier for the gas to escape the channel from the top. And finally, the slug flow pattern is formed at the end of the channel, when the liquid slug envelopes the whole channel cross section.

These selected four cases also imply that, the flow patterns in a longer PEM fuel cell flow channel may also follow this flow pattern evolution along the channel length, namely, bottom corner flow at the beginning of channel, followed by bottom and top corner flow, annular flow, and finally slug flow at the end of channel.

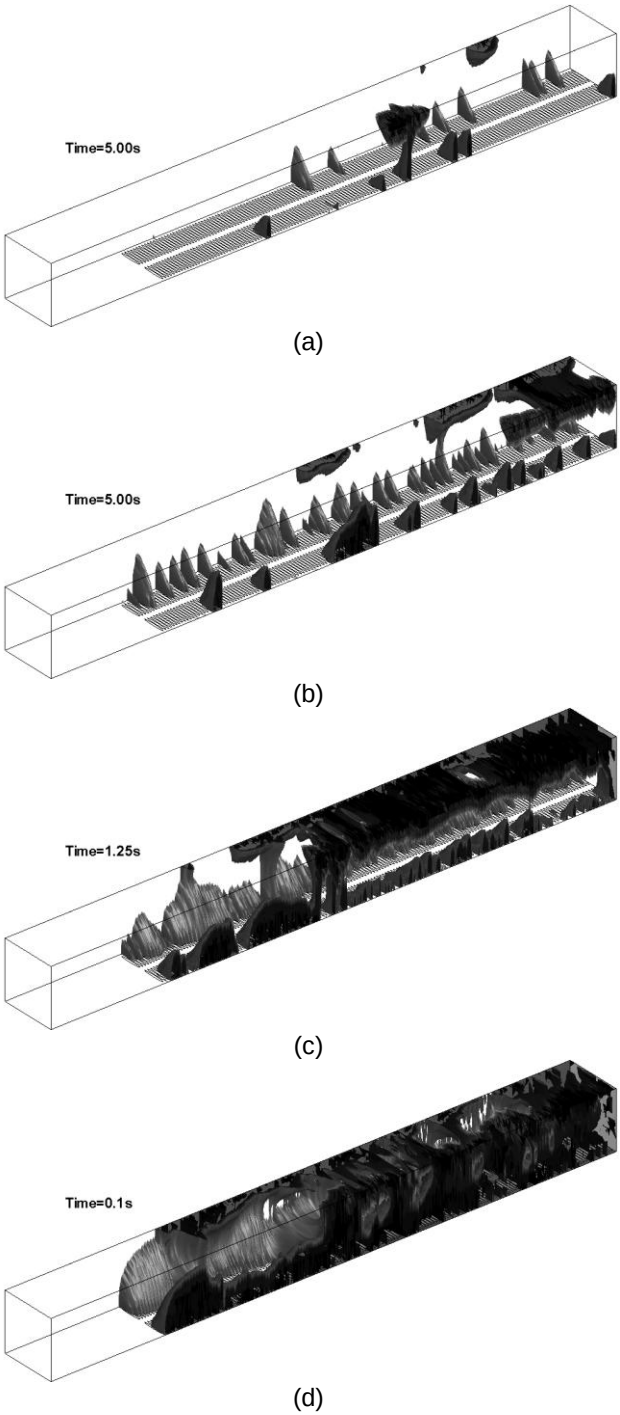

Figure 5. Effects of liquid flow rate on the two-phase flow patterns in the minichannel: (a) base case, (b) 10x case, (c) 100x case, and (d)1000x case.

To quantitatively analyze the effects of liquid flow rates on two-phase flow patterns, the time-averaged water coverage ratio on different walls, water volume fraction and pressure drop were calculated for the four cases. The water coverage ratio is defined as the ratio of the surface area covered by water to the total surface area. In PEM fuel cells, reactants diffuse through the GDL. Hence, the GDL surface water coverage ratio is a key parameter that indicates the negative effects of liquid water on PEM fuel cell performance. The water volume fraction or degree of saturation indicates the degree of channel flooding. The pressure drop, which is another important parameter, indicates the energy loss of fluid flowing through the channel. For operating PEM fuel cells, a lower GDL surface water coverage ratio, a lower water fraction, and a lower parasitic pressure loss are preferred.

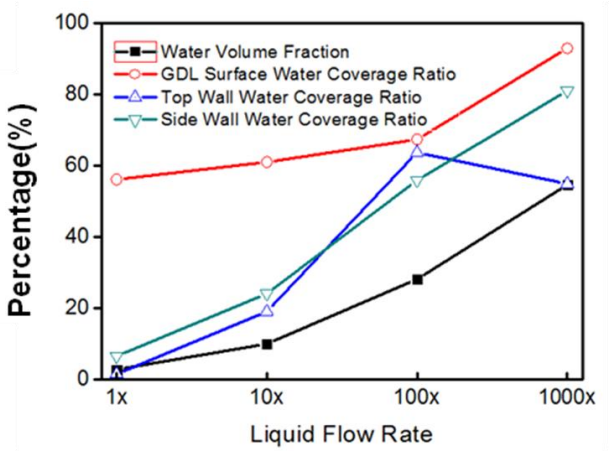

Figure 6. Effects of liquid flow rate on the water distribution in the minichannel.

Theoretically, increasing liquid flow rate results in higher water volume fraction and higher water coverage ratio. However, as shown in the Figure , the 1000x case has lower top wall water coverage ratio but much higher GDL surface water coverage ratio compared to the 100x case. As discussed previously, when slug flow occurs, it is easier for the gas to flow above the water, which decreases the top wall coverage ratio but increases the GDL surface coverage ratio.

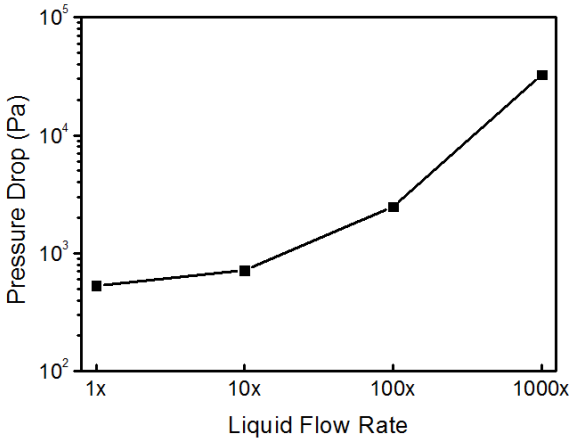

Figure 7. Effects liquid flow rate on the pressure drop in the minichannel.

Effects of liquid flow rate on the time-averaged pressure drop is shown in **Error! Reference source not found.**. It is

found that when the flow approaches the slug flow, the pressure drop rapidly increases. All the above results suggest that, in practice, the slug flow pattern in the PEM fuel cell flow channel should be avoided to decrease the GDL surface water coverage and pressure drop.

In the flowing sections, the effects of material wettabilities are investigated. In order to shorten the huge computational time, the 10x case is used as a reference case, since it has very similar flow pattern as the base case and it is also a reasonable flow rate when the water condensation rate is considered.

Effects of GDL surface wettabilities

The wettability of the GDL, which is characterized by the surface contact angle, can be altered by varying the PTFE contents in the GDL. The effects of GDL surface wettability on the two-phase flow pattern in the minichannel were investigated by varying the GDL surface static contact angle from 45^o to 140^o i.e., 45^o, 60^o, 90^o, 120^o, and 140^o. Figure 8 shows different two-phase flow patterns in the channel for different GDL wettabilities. When the GDL surface contact angle is hydrophilic, i.e. the contact angle is less than 90^o (Figure 8a, b, c), a thin liquid film is formed on the GDL surface, which blocks the diffusion pathway of reactants (air gas) to the catalyst layer, leading to decreased fuel cell performance. As the contact angle of GDL surface increases, liquid water begins to move to and accumulate on the side walls and the higher a contact angle, the more water moves from GDL surface to side walls. When GDL surface is hydrophobic, i.e. the contact angle is more than 90^o (Figure 8d, e), the flow pattern is corner flow as observed in the base case.

Figure 9 shows that hydrophobic and hydrophilic GDL surfaces show very different liquid distribution profiles. For the hydrophilic GDL surface, the water coverage ratio on the side walls changes very little with varying GDL contact angle, and no water is present on the top wall, with the water coverage ratio on the GDL surface decreasing significantly as the contact angle increases. That is because a higher contact angle lifts the water up, i.e., move it from a film to a droplet, which is more conducive to water removal from the GDL surface. For the hydrophobic GDL surface, increasing its contact angle further decreases the water coverage ratio on the GDL surface. Meanwhile the liquid droplets are able to touch the top wall, resulting in the top corner flow, which decreases the water coverage ratio on the side walls and also reduces the total water volume fraction in the channel, due to the fast movement of droplets in the top corners.

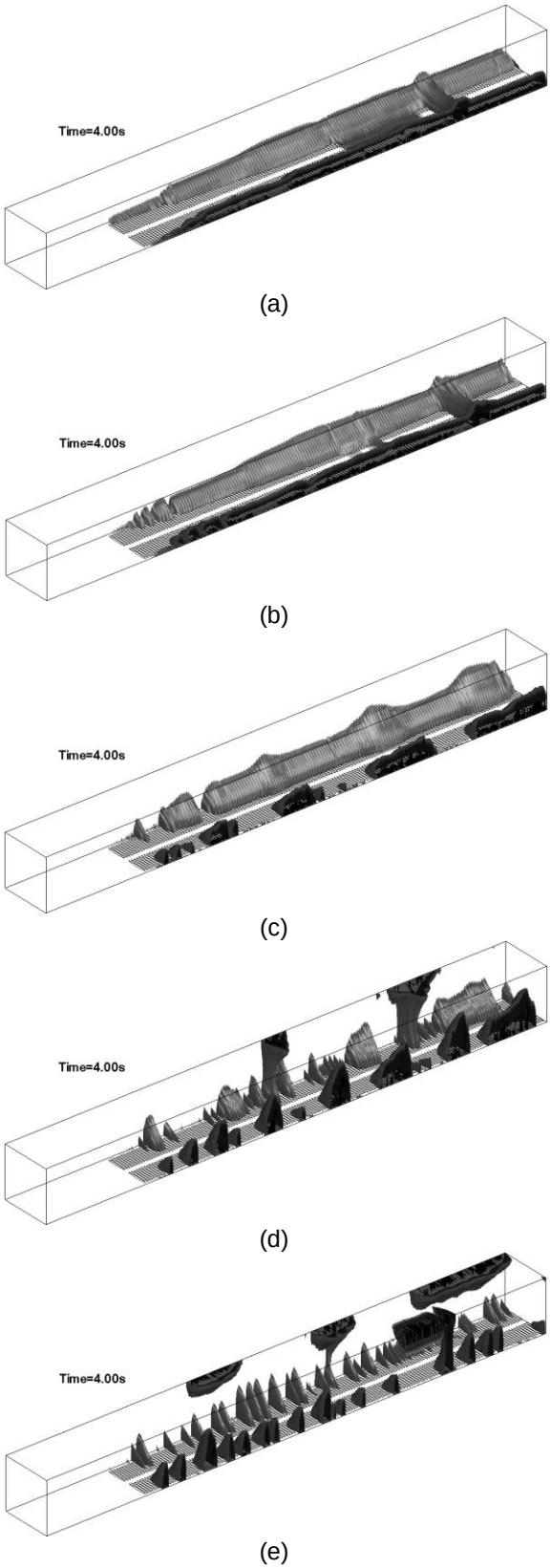

Figure 8. Effects of contact angle of GDL surface on the two-phase flow patterns in the minichannel:(a) $\theta=45^o$, (b) $\theta=60^o$,(c) $\theta=90^o$, (d) $\theta=120^o$, (e) $\theta=140^o$.

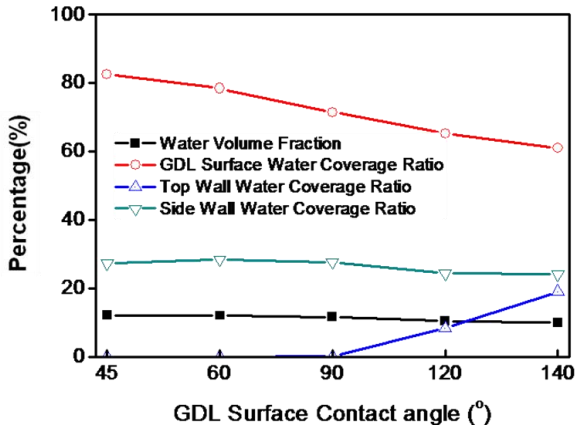

Figure 9. Effects of contact angle of GDL surface on the water distribution in the minichannel.

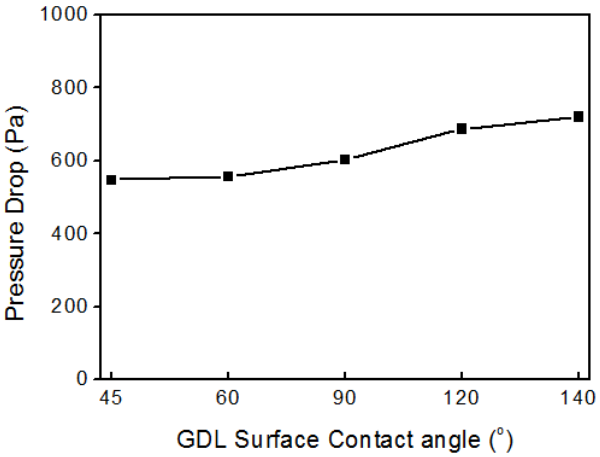

Figure 10. Effects of contact angle of GDL surface on the pressure drop in the minichannel.

The effects of GDL surface wettability on the time-averaged pressure drop is shown in Figure 10. It is seen that increasing the GDL surface contact angle always increases the total pressure drop. This is because more hydrophobicity of GDL surface lifts up the water more from the GDL surface to occupy more cross sectional channel area, which blocks the gas pathway in the channel, resulting in higher pressure drop.

It can be concluded from the above observation that increasing the hydrophobicity of the GDL surface is helpful to expel liquid water from the GDL surface and also to reduce the water fraction in the channel, but the pressure drop increases slightly. Since the wettability of the GDL also affects the water transport inside the GDL, and the balance between avoiding flooding and reducing parasitic energy loss depends on specific applications. Therefore, it is difficult to conclude which contact angle should be the optimal for the PEM fuel cell performance.

Effects of channel wall surface wettabilities

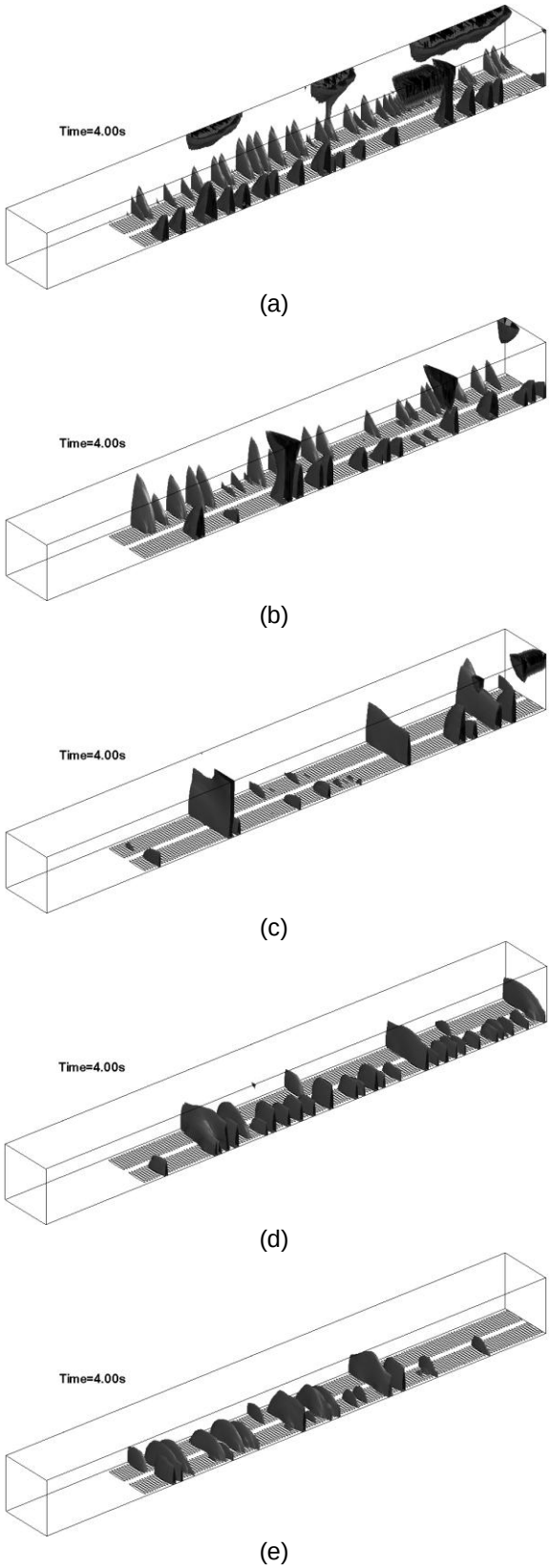

Figure 5. Effects of contact angle of channel side and top wall surfaces on the two-phase flow patterns in the minichannel: (a) θ=45°, (b) θ=60°,(c) θ=90°, (d) θ=120°, (e) θ=140°.

Instead of changing the GDL surface wettability, one can also change the channel wall wettability for a given GDL to improve the water management in the gas channel. The effects of channel wall surface wettability were investigated by varying the contact angle of channel wall from 45° to 140°. Figure 5 shows the effects of different wall surface contact angles, i.e., 45°, 60°, 90°, 120°, and 140°, on the two-phase flow patterns in the channel. For hydrophilic wall surfaces, the flow pattern is in corner flow as observed in the base case. More hydrophilic wall surfaces make the droplet on the bottom corner easier to move to the top wall. For hydrophobic wall surfaces, the flow pattern is in droplet flow on the GDL surface, and more hydrophobic wall surface prevents the formation of big droplets.

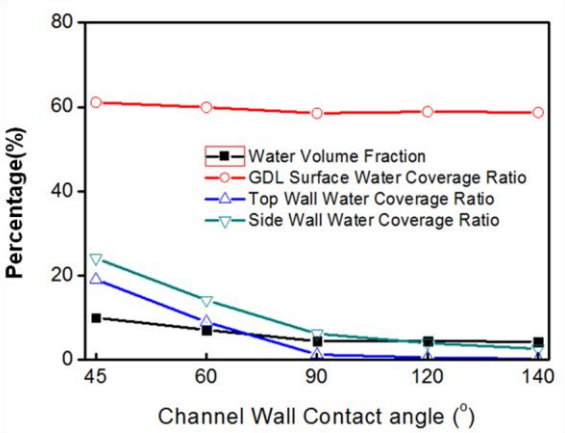

Figure 6. Effects of contact angle of channel side and top wall surfaces on the water distribution in the minichannel.

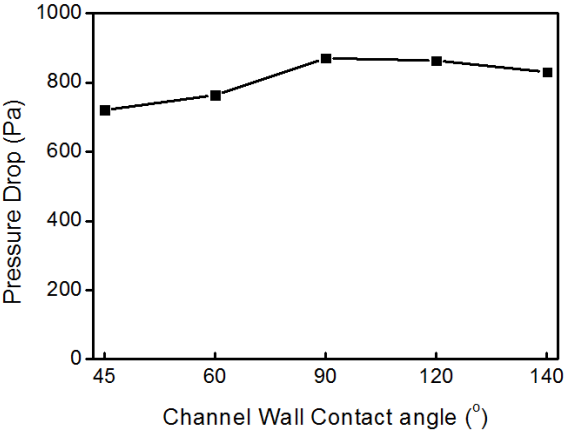

Figure 7. Effects of contact angle of channel side and top wall surfaces on the pressure drop in the minichannel.

The effects of channel side and top wall surface wettability on the water distribution is shown in Figure 6. It is found that when the channel wall is hydrophilic, increasing the channel wall contact angle significantly decreases the water coverage ratio on the top and side walls, due to its preventing the droplet formation on the side walls. Correspondingly, the GDL surface coverage and water volume fraction also decrease slightly, since larger droplets can be formed on the GDL surface, which accelerates water removal from the channel. When the channel wall is hydrophobic, stable droplet flow is formed, with little water on the top and side walls. Therefore, further increasing channel wall contact angle has little impact on the water distribution in the channel.

The effect of channel wall surface wettability on the pressure drop is shown in Figure 7. It is found that the pressure drop increases first with increasing the channel wall contact angle due to the less water on the top wall, and then decreases due to the formation of smaller droplets on the GDL surface, as shown in Figure 5. The above results suggest that more hydrophilic channel wall should be always used to reduce the water volume fraction in the channel to reduce the parasitic energy loss.

CONCLUSIONS

The following conclusions can be drawn from this study:

1) Using a simplified microstructure of GDL surface, three stages of two-phase flow patterns, namely emergence and merging of liquid water on the GDL surface, accumulation on the side walls, and detachment from the top wall, can be identified when liquid water is injected through the GDL into a minichannel. For the base case, the flow pattern is in corner flow, mostly in the bottom corners and sometimes in the top corners.

2) With increasing the liquid injection rates, the flow pattern evolves from the bottom corner flow to top and bottom corner flow, annular flow, and finally slug flow. And the slug flow should be avoided in PEM fuel cells, since it causes extremely high GDL coverage and high pressure drop.

3) The material wettabilities have a great impact on the two-phase flow pattern, water distribution and pressure drop. Using more hydrophobic GDL surface is helpful to expel water from the GDL surface, but also increases the pressure drop. On the other hand, more hydrophilic side and top channel walls facilitate the water removal and reduce the pressure drop.

ACKNOWLEDGMENTS

The authors are grateful to the Natural Science and Engineering Research Council of Canada (NSERC) for a Strategic Grant to support this study.

REFERENCES

1. Anderson, R., et al., *A critical review of two-phase flow in gas flow channels of proton exchange membrane fuel cells.* Journal of Power Sources, 2010. **195**(15): p. 4531-4553.

2. Weber, A.Z., et al., *Modeling transport in polymer-electrolyte fuel cells.* Chemical Reviews, 2004. **104**(10): p. 4679-4726.
3. Um, S., et al., *Computational fluid dynamics modeling of proton exchange membrane fuel cells.* Journal of The Electrochemical Society, 2000. **147**(12): p. 4485-4493.
4. Mazumder, S., et al., *Rigorous 3-D Mathematical Modeling of PEM Fuel Cells.* Journal of The Electrochemical Society, 2003. **150**(11): p. A1503-A1509-A1503-A1509.
5. Theodorakakos, A., et al., *Dynamics of water droplets detached from porous surfaces of relevance to PEM fuel cells.* Journal of Colloid and Interface Science, 2006. **300**(2): p. 673-687.
6. Zhan, Z., et al., *Characteristics of droplet and film water motion in the flow channels of polymer electrolyte membrane fuel cells.* Journal of Power Sources, 2006. **160**(1): p. 1-9.
7. Shirani, E., et al., *Deformation of a Droplet in a Channel Flow.* Journal of Fuel Cell Science and Technology, 2008. **5**(4): p. 041008-8.
8. Cai, Y.H., et al., *Effects of hydrophilic/hydrophobic properties on the water behavior in the micro-channels of a proton exchange membrane fuel cell.* Journal of Power Sources, 2006. **161**(2): p. 843-848.
9. Zhu, X., et al., *Dynamic behaviour of liquid water emerging from a GDL pore into a PEMFC gas flow channel.* Journal of Power Sources, 2007. **172**(1): p. 287-295.
10. Bazylak, A., et al., *Dynamic water transport and droplet emergence in PEMFC gas diffusion layers.* Journal of Power Sources, 2008. **176**(1): p. 240-246.
11. Zhu, X., et al., *Numerical simulation of emergence of a water droplet from a pore into a microchannel gas stream.* Microfluidics and Nanofluidics, 2008. **4**(6): p. 543-555.
12. Zhu, X., et al., *Three-dimensional numerical simulations of water droplet dynamics in a PEMFC gas channel.* Journal of Power Sources, 2008. **181**(1): p. 101-115.
13. Fang, C., et al., *3-D numerical simulation of contact angle hysteresis for microscale two phase flow.* International Journal of Multiphase Flow, 2008. **34**(7): p. 690-705.
14. Quan, P., et al., *Water behavior in serpentine micro-channel for proton exchange membrane fuel cell cathode*. Journal of Power Sources, 2005. **152**: p. 131-145.
15. Jiao, K., et al., *Liquid water transport in parallel serpentine channels with manifolds on cathode side of a PEM fuel cell stack.* Journal of Power Sources, 2006. **154**(1): p. 124-137.
16. Jiao, K., et al., *Liquid water transport in straight micro-parallel-channels with manifolds for PEM fuel cell cathode.* Journal of Power Sources, 2006. **157**(1): p. 226-243.
17. Quan, P., et al., *Numerical study of water management in the air flow channel of a PEM fuel cell cathode.* Journal of Power Sources, 2007. **164**(1): p. 222-237.
18. Le, A.D., et al., *A general model of proton exchange membrane fuel cell.* Journal of Power Sources, 2008. **182**(1): p. 197-222.
19. Le, A.D., et al., *Fundamental understanding of liquid water effects on the performance of a PEMFC with serpentine-parallel channels.* Electrochimica Acta, 2009. **54**(8): p. 2137-2154.
20. Ding, Y., et al. *3-D numerical simulation of water droplet emerging from a non-uniform gas diffusion layer surface*. in *The 20th International Symposium on Transport Phenomena*. 2009. Victoria BC, CANADA.
21. Litster, S., et al., *Two-phase transport in porous gas diffusion electrodes*, in *Transport phenomena in fuel cells*, B. Sunden and M. Faghri, Editors. 2005, WIT Press. p. 175-213.
22. *FLUENT 6.3 User's Guide 2006, Fluent Inc.*